UNCLASSIFIED

SECURITY CLASSIFICATION OF THIS PAGE

REPORT DOCUMENTATION PAGE

1a. REPORT SECURITY CLASSIFICATION UNCLASSIFIED	1b. RESTRICTIVE MARKINGS
2a. SECURITY CLASSIFICATION AUTHORITY	3. DISTRIBUTION / AVAILABILITY OF REPORT Approved for public release; distribution unlimited.
2b. DECLASSIFICATION / DOWNGRADING SCHEDULE	
4. PERFORMING ORGANIZATION REPORT NUMBER(S) NUSC TD 7399	5. MONITORING ORGANIZATION REPORT NUMBER(S)
6a. NAME OF PERFORMING ORGANIZATION Naval Underwater Systems Center 6b. OFFICE SYMBOL (If applicable) 3331	7a. NAME OF MONITORING ORGANIZATION
6c. ADDRESS (City, State, and ZIP Code) New London Laboratory New London, CT 06320	7b. ADDRESS (City, State, and ZIP Code)
8a. NAME OF FUNDING / SPONSORING ORGANIZATION Naval Sea Systems Command 8b. OFFICE SYMBOL (If applicable) SEA63R	9. PROCUREMENT INSTRUMENT IDENTIFICATION NUMBER
8c. ADDRESS (City, State, and ZIP Code) Arlington, VA	10. SOURCE OF FUNDING NUMBERS PROGRAM ELEMENT NO. PE62711 / PROJECT NO. SF11123 / TASK NO. / WORK UNIT ACCESSION NO.

11. TITLE (Include Security Classification)
EFFECTS OF ACOUSTIC MULTIPATH INTERACTIONS ON SOURCE RANGE AND BEARING ESTIMATION FOR A FOCUSED LINE ARRAY

12. PERSONAL AUTHOR(S)
Joseph M. Monti and Paul D. Koenigs

13a. TYPE OF REPORT	13b. TIME COVERED FROM ____ TO ____	14. DATE OF REPORT (Year, Month, Day)	15. PAGE COUNT
		1985 May 24	16

16. SUPPLEMENTARY NOTATION
A paper presented at the 109th meeting of the Acoustical Society of America, 8-12 April 1985, Austin, Texas

17 COSATI CODES			18. SUBJECT TERMS (Continue on reverse if necessary and identify by block number)
FIELD	GROUP	SUB-GROUP	Acoustic Multipath; Bearing Estimation; Beamforming; Focused Beamforming; Bearing Error; Focused Line Array

19. ABSTRACT (Continue on reverse if necessary and identify by block number)

A computer simulation technique was developed to investigate the effects of acoustic multipath interactions on source range and bearing estimation for a focused line array. To simulate the multipath environment, the Generic Sonar Model (Weinberg, NUSC TD 5971, 19 December 1981) was used to modify source signals and emulate oceanic transmissions to individual sensors. Characteristics of a narrowband frequency domain focused beamformer were implemented incorporating wavefront curvature techniques and a maximum-likelihood estimator. Simulations for sparsely populated colinear arrays were conducted at several frequencies for differing sound speed profiles, bottom loss conditions, and source/receiver configurations. The beamformer output was used to obtain relative array pressure response and analyzed to obtain source range and bearing estimation errors. For a given environmental case the results indicate no bearing and relatively small range errors for a source located at broadside for the simulated range and frequency parameters.

20. DISTRIBUTION / AVAILABILITY OF ABSTRACT ☐ UNCLASSIFIED/UNLIMITED ☒ SAME AS RPT. ☐ DTIC USERS	21. ABSTRACT SECURITY CLASSIFICATION Unclassified
22a. NAME OF RESPONSIBLE INDIVIDUAL Joseph M. Monti	22b. TELEPHONE (Include Area Code) (203) 440-4859 22c. OFFICE SYMBOL 3331

DD FORM 1473, 84 MAR 83 APR edition may be used until exhausted. All other editions are obsolete.

SECURITY CLASSIFICATION OF THIS PAGE

UNCLASSIFIED

19. Continued:

Bearing and range estimates degrade as the source moves to off-broadside locations. For a given source/receiver geometry, the results indicate range and bearing errors can be dependent on the environment due to the resulting complexity of the multipath structure.

18. Continued:

Frequency Domain Beamforming
Maximum-Likelihood Estimation
Multipath Interaction
Range Error
Range Estimation
Source Localization
Source Localization Errors
Wavefront Curvature

NUSC Technical Document 7399
24 May 1985

Effects of Acoustic Multipath Interactions on Source Range and Bearing Estimation for a Focused Line Array

A Paper Presented at the 109th Meeting of the Acoustical Society of America, 8-12 April 1985, Austin, Texas

Joseph M. Monti
Paul D. Koenigs
Surface Ship Sonar Department

Naval Underwater Systems Center
Newport, Rhode Island / New London, Connecticut

PREFACE

This document was prepared under NUSC Project No. A65400, "Towed Array Sonar Technology (TAST)," NUSC Program Manager, Dr. N. L. Owsley (Code 3211). The sponsoring activity is the Naval Sea Systems Command, C. D. Smith (NAVSEA 63R). Funding was provided under program element 62711N, D. Porter (NAVSEA 63R3).

REVIEWED AND APPROVED: 24 May 1985

Larry Freeman
Head: Surface Ship Sonar Department

The authors of this document are located at the New London Laboratory, Naval Underwater Systems Center, New London, CT 06320.

EFFECTS OF ACOUSTIC MULTIPATH INTERACTIONS ON
SOURCE RANGE AND BEARING ESTIMATION FOR A
FOCUSED LINE ARRAY

-- First viewgraph, please. --

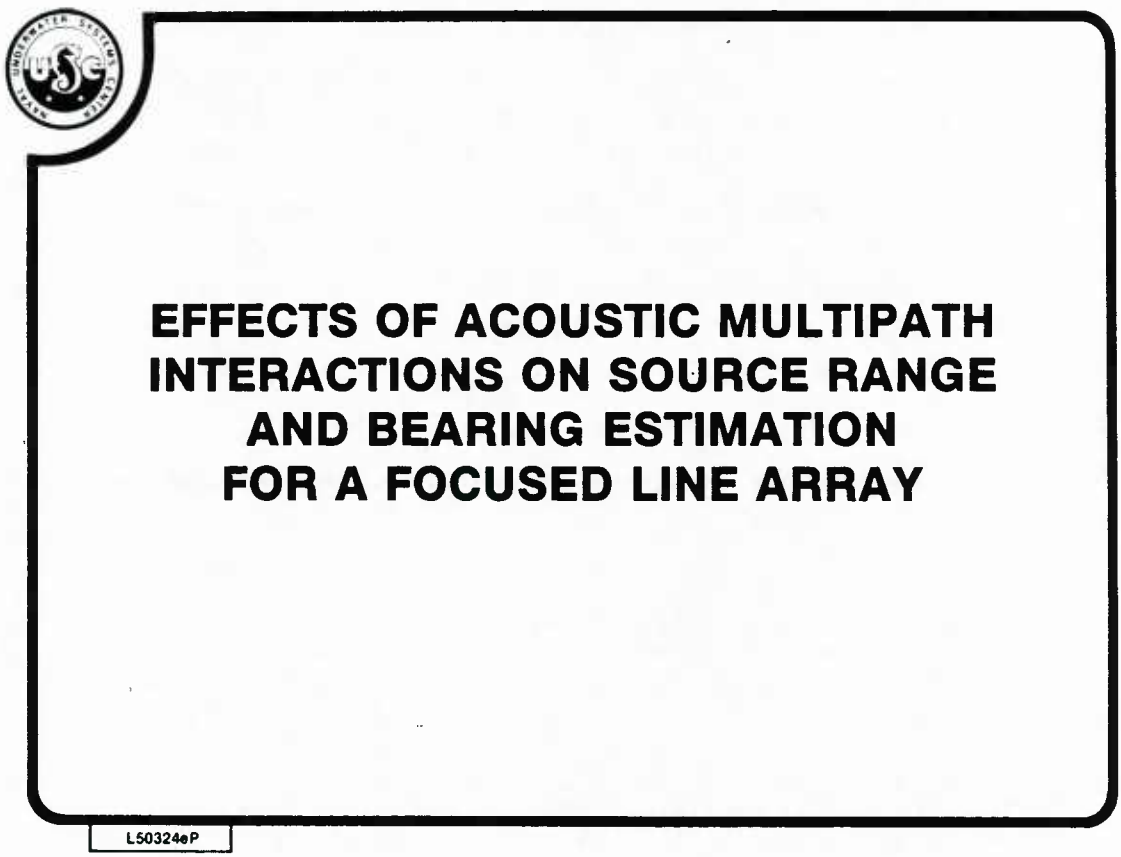

Viewgraph 1

To solve the problem of source range and bearing estimation for passive localization, the differences in signal arrivals within an array of sensors must be examined. Previous investigations have addressed single plane wave [1], single spherical wave [2,3], and idealized multipath spherical wave [4] propagation. The present study extends these theoretical investigations to include complex multipath propagation conditions that can arise from acoustic transmissions through an oceanic environment.

It is known that source range and bearing estimates based on acoustic arrival times are susceptible to error if the effects of multipath transmissions are neglected. Furthermore, the use of multipath propagation conditions can serve to improve the accuracy of range and bearing estimations [4].

-- Next viewgraph, please. --

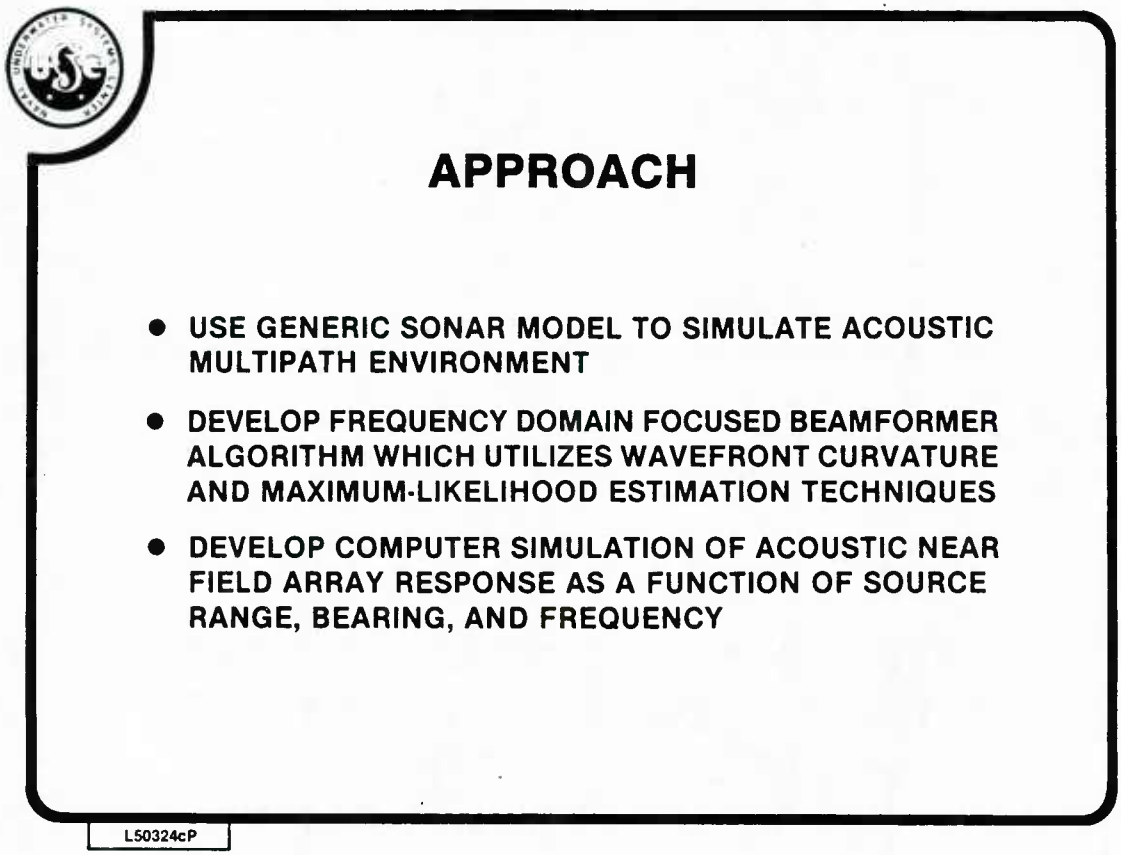

Viewgraph 2

The approach consisted basically of three steps. First, to simulate the acoustic multipath environment and source and receiver characteristics, the Generic Sonar Model [5] was used. Second, a frequency domain focused beamforming algorithm was developed that uses wavefront curvature and maximum-likelihood estimation techniques. Finally, a frequency domain focused beamformer simulation was used to obtain relative array beam power output as a function of frequency, bearing, and range for a given source location. The beam power output functions were then used to obtain estimates of source location and range and bearing errors.

-- Next viewgraph, please. --

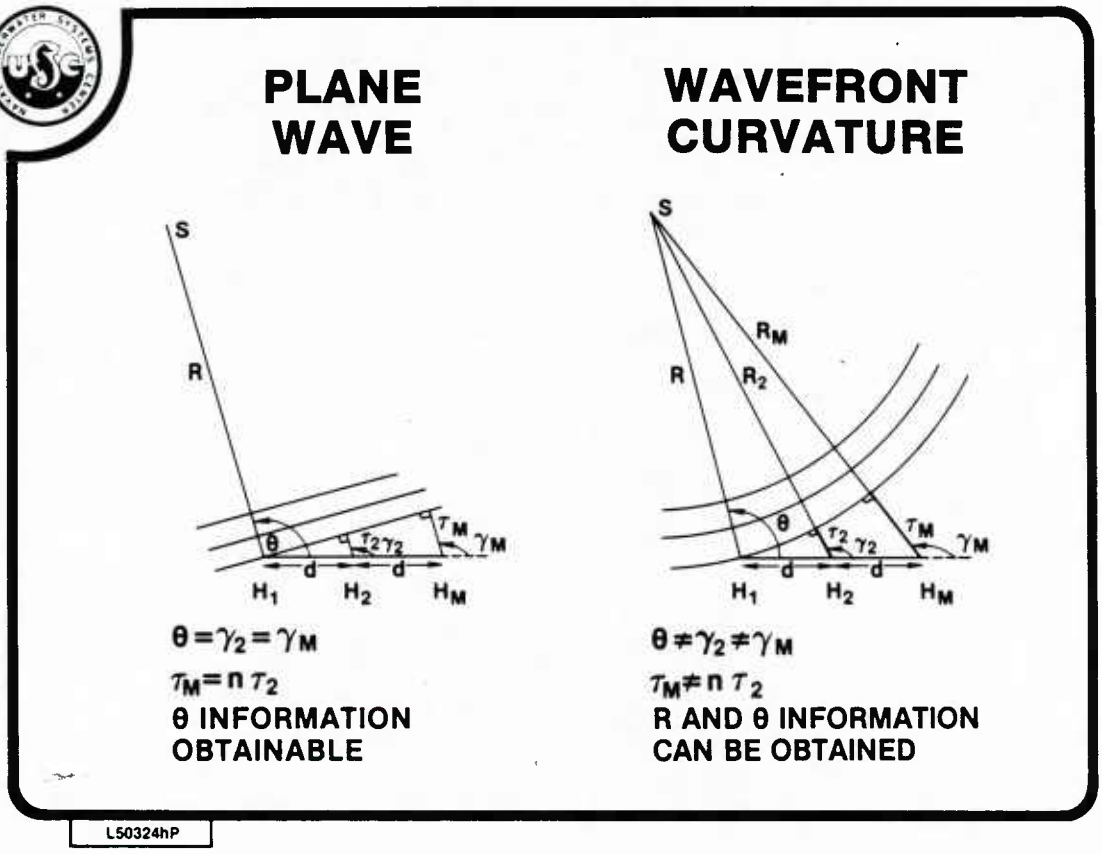

Viewgraph 3

Consider a line array of M equispaced hydrophones as presented here. Note that the range R and bearing θ of the source is relative to hydrophone 1 (H_1). The range is the horizontal range between source and hydrophone 1 and the bearing angle is measured as the angle between the positive X axis and hydrophone 1.

The differences that occur when an array of sensors encounters a propagating plane wave as compared to wavefront curvature propagation are shown in viewgraph 3. In the case of a propagating plane wave, the time delays τ_2 and τ_3 are linearly related by the Pythagorean theorem. It should also be noted that in the plane wave propagation case the angles γ_2 and γ_M are the same angle and are equal to the bearing angle θ. In the case of wavefront curvature propagation, the time delays necessary for array focusing are not linearly related, but are instead related by the law of cosines. Also, γ_2 and γ_M are not equal and neither angle is equal to the bearing angle θ. Finally, only bearing information can be obtained using plane wave techniques whereas range and bearing information can be obtained using wavefront curvature techniques.

-- Next viewgraph, please. --

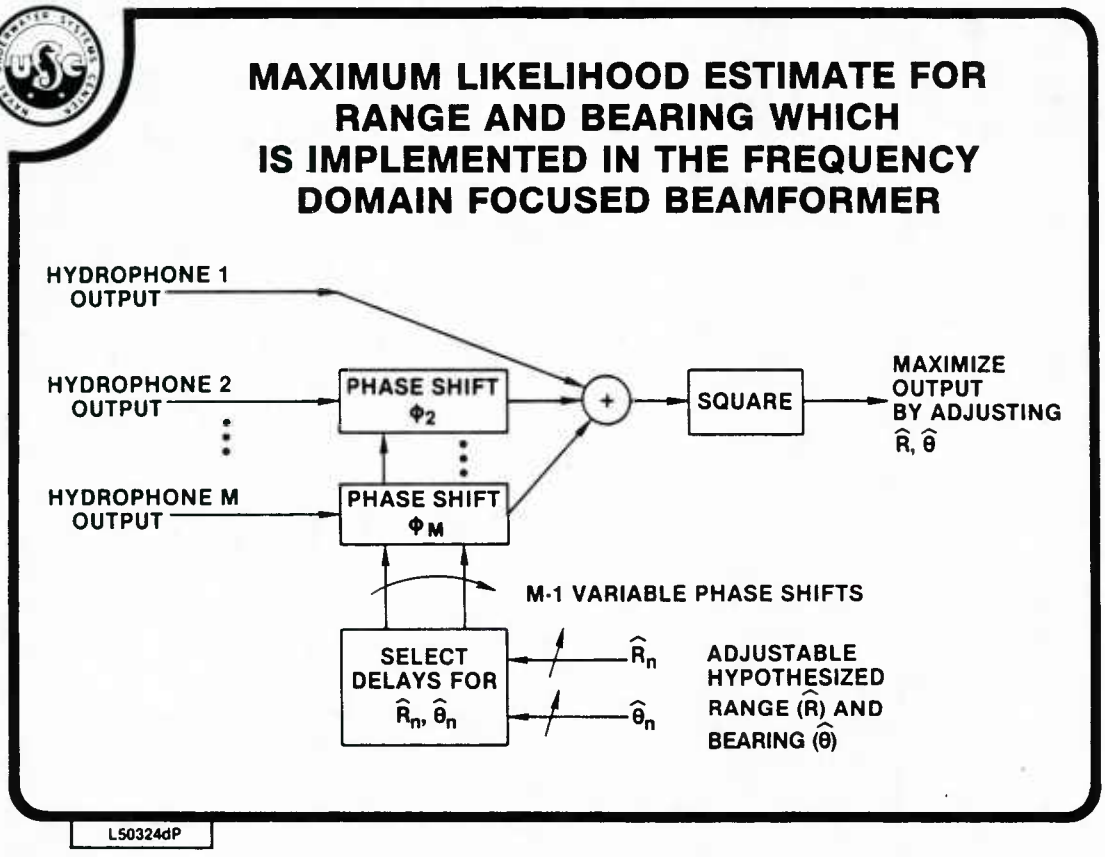

Viewgraph 4

The frequency domain focused beamforming technique used is based on a maximum-likelihood estimation process [4] as illustrated here. The hydrophone outputs consist of a complex signal that is the result of a coherent addition of all possible acoustic paths between the source and the receiver of interest for a given frequency. In the next step an assumption is made that an approximate source range and bearing is known and estimates of range ($\hat{R}$) and bearing ($\hat{\theta}$) are then simulated to find the maximum output of the focused beamformer. This is accomplished by hypothesizing a set of range estimates ($\hat{R}_n$) and bearing estimates ($\hat{\theta}_n$) for implementation in the maximum-likelihood estimator. The appropriate time delays for M hydrophones are then calculated for each directional vector. The time delays that are computed are actually phase delays (ϕ_m) in the frequency domain.

When the magnitude squared of the beamformer output is maximized with respect to $\hat{R}_n$ and $\hat{\theta}_n$, the estimated values of $\hat{R}_n$ and $\hat{\theta}_n$ that correspond to this maximum are the values that represent the estimated horizontal range and bearing of the source in a maximum-likelihood sense.

-- Next viewgraph, please. --

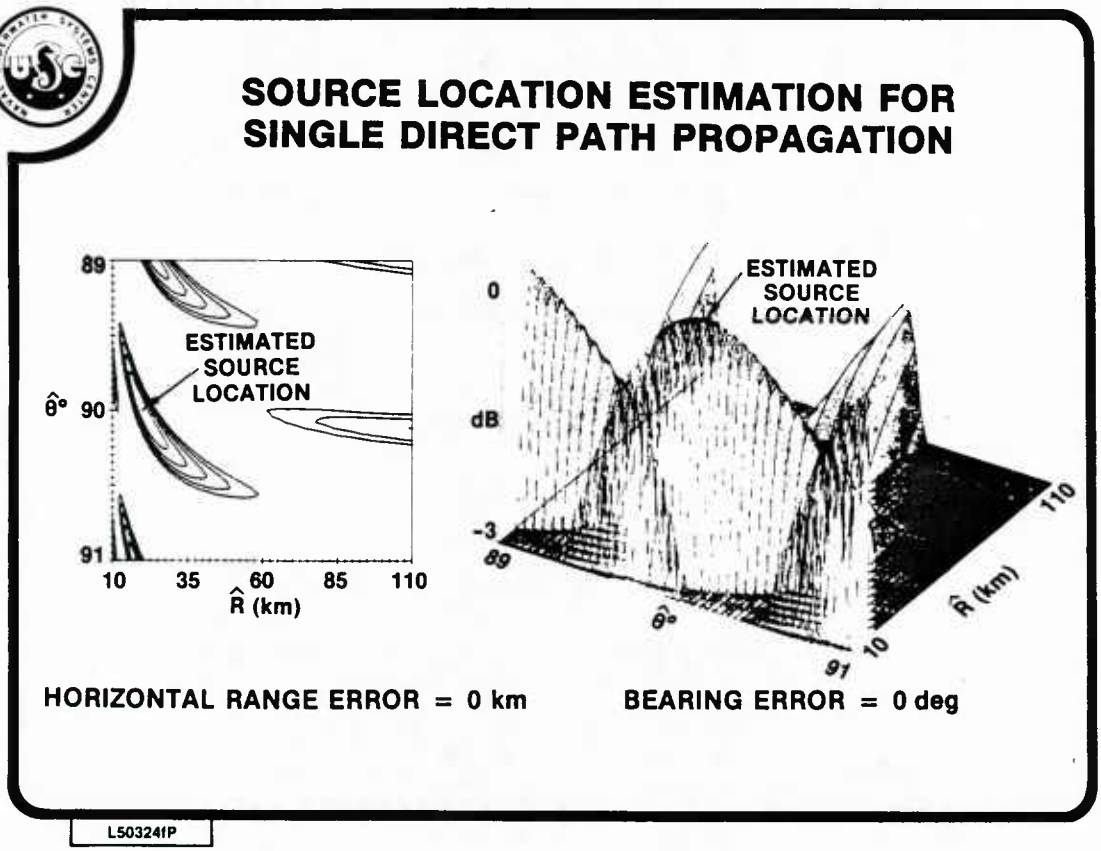

Viewgraph 5

The first scenario is for a source located at 20 kilometers and 90 degrees relative to the reference hydrophone H_1. When the beamformer simulation is employed, it focuses on a source at the proper range of 20 kilometers and a bearing of 90 degrees. The focused beamformer algorithm is based on a maximum-likelihood estimator process. The peak value is chosen from all possible values. Here, the peak selection process is done over a range-bearing surface, which can contain ambiguities in range and/or bearing. A three-dimensional representation of the estimator outputs is shown here. All values plotted are within 3 dB of the peak value. Note the ambiguities in range and bearing and the number of peaks within 3 dB of the true peak. As can be seen, it is very difficult to find the true peak in this type of representation. For this reason a contour plot of the data in 0.5 dB intervals is also presented. The source is easily spotted here and is represented as a dot at 20 kilometers and 90 degrees.

The character of the contoured viewgraph can be explained by examining the near field behavior of a continuous line array. Based on Steinberg's [6] development, the hyperfocal range for this array is nearly the same as the source range. Thus, we can relate the closed contours to the array's depth of field. The skewness is simply due to our selection of the first sensor as the center of the coordinate system.

-- Next viewgraph, please. --

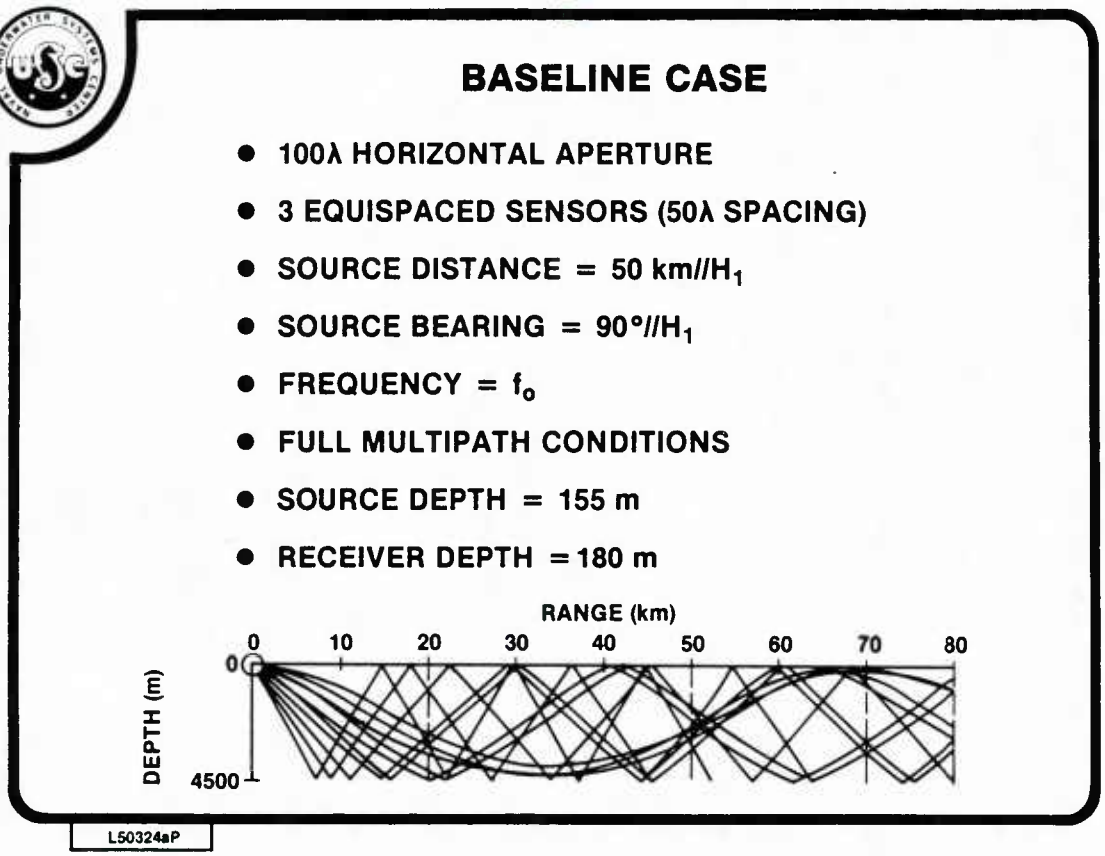

Viewgraph 6

The ocean environment was simulated using the Generic Sonar Model. A historic North Atlantic sound speed profile and water depth were utilized. An illustration of the ray trace is presented here. Also, the parameters that establish our baseline case are shown. The baseline case consists of three omnidirectional equispaced sensors with an associated elemental spacing of 50λ at f_o. The omnidirectional source is located at a horizontal range of 50 kilometers and a bearing of 90 degrees relative to hydrophone 1. Our baseline case is for a source depth of 155 meters and a receiver depth of 180 meters.

-- Next viewgraph, please. --

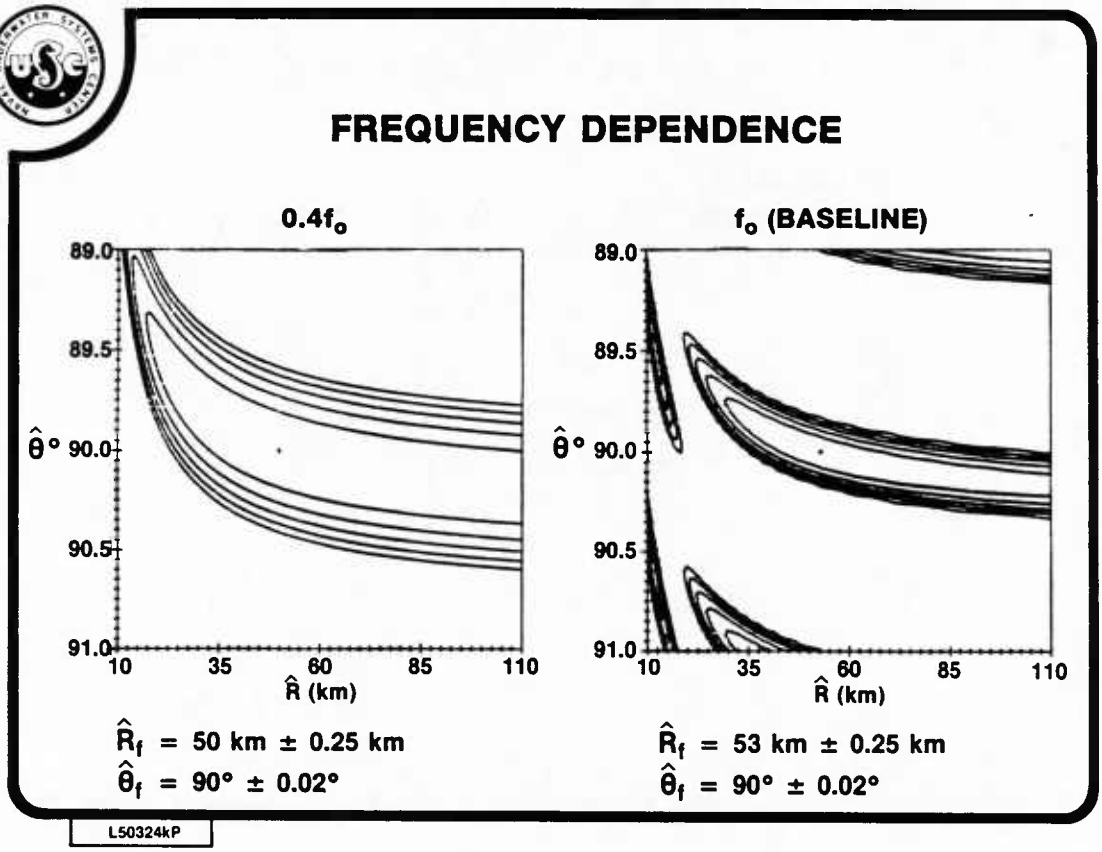

Viewgraph 7

This viewgraph represents contours of the estimators at two frequencies for a source range of 50 kilometers and bearing of 90 degrees. The baseline frequency is shown on the right and a lower frequency of $0.4f_o$ is shown on the left. It is apparent that as the frequency is decreased, the ambiguous or aliased surfaces spread out in bearing. This is the same effect one sees when analyzing beam patterns for sparsely populated arrays. Thus, the introduction of multipath differences occurring at these two frequencies has little impact on the general character of the contours. However, the location of the local maximum for the lower frequency now coincides with the actual range.

-- Next viewgraph, please. --

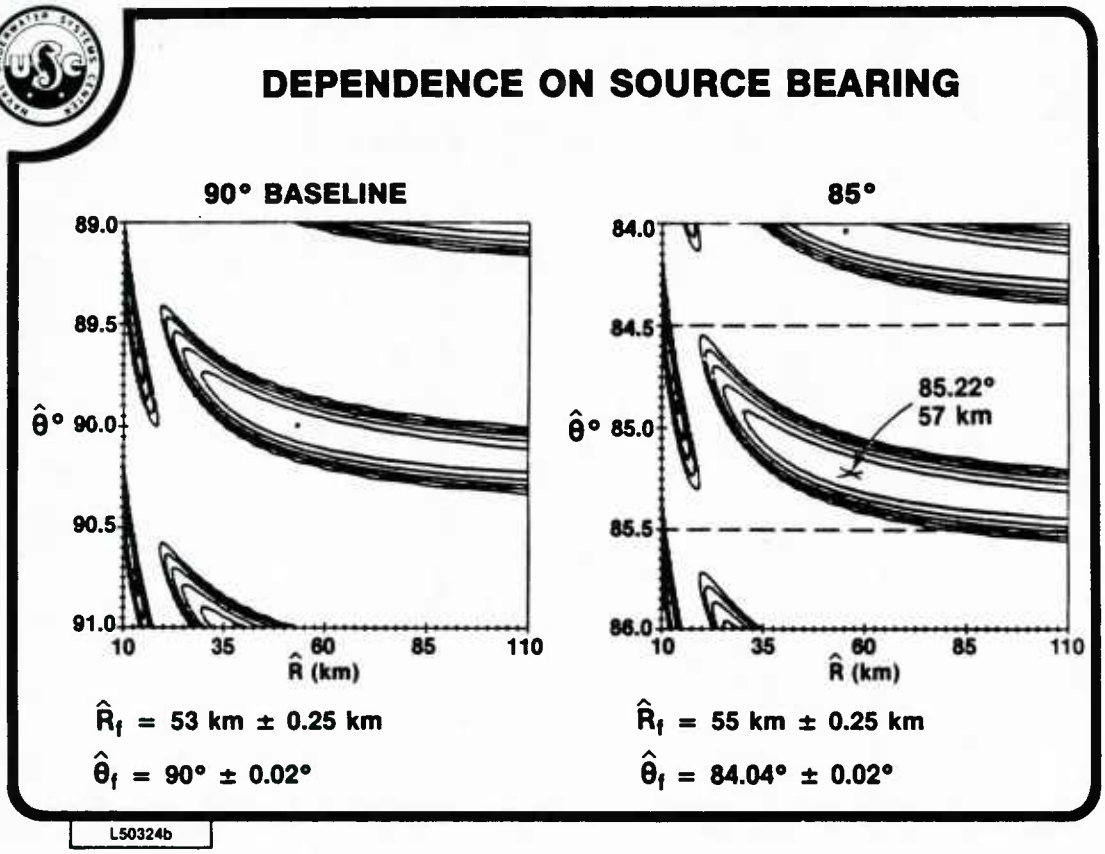

Viewgraph 8

The dependence on source bearing relative to the first sensor is presented here. The broadside case is shown on the left. When the source is located at 50 kilometers and bearing is 85 degrees, the maximum estimator value within the grid is shown (by a dot near the top) at a range of 55 kilometers. It is obvious in this case that the wrong local maximum was selected. If the search area is reduced as shown by the dashed lines, so that all aliased responses are excluded, the maximum is located at 57 kilometers and a bearing of 85.2 degrees. This point is shown by an X in this viewgraph. Thus we can see a degradation in range and bearing estimates for sources located only slightly off broadside.

--Next viewgraph, please. --

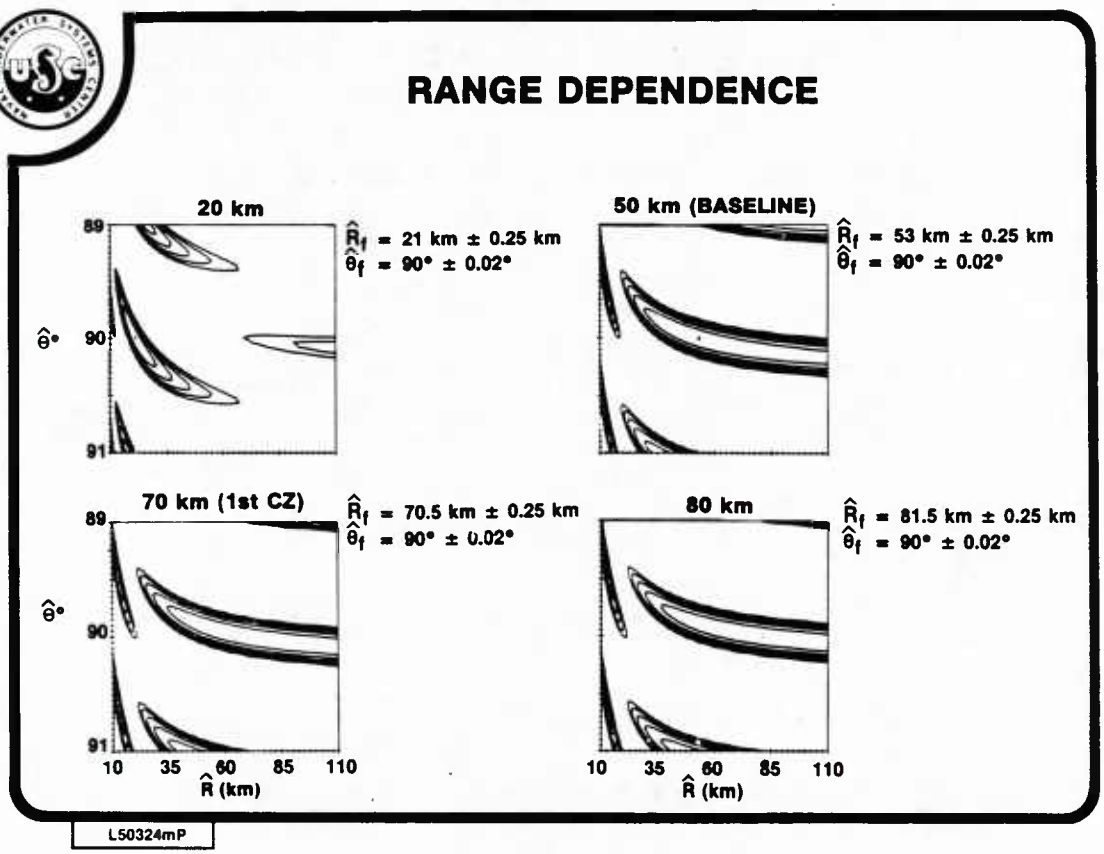

Viewgraph 9

Here we can see the dependence of the estimator outputs on source range when the source bearing is 90 degrees. The actual source ranges are given at the top of each viewgraph and the local maximum range and bearing estimators are to the right. We can see that in general there is no bearing error, and, despite the fact that we have gone from single bottom bounce through convergence zone to double bottom bounce principal modes of propagation, the estimated ranges are still quite accurate. We note the character of the results for the 20 kilometer case is substantially different than the other cases. As mentioned earlier this is principally due to the relationship between the arrays hyperfocal range and the source range. For this array the hyperfocal range is approximately 20 kilometers. Thus, we can expect a significant decrease in estimator outputs as range increases. Therefore, we have a closed contour at 20 kilometers, but not for the remaining cases.

-- Next viewgraph, please. --

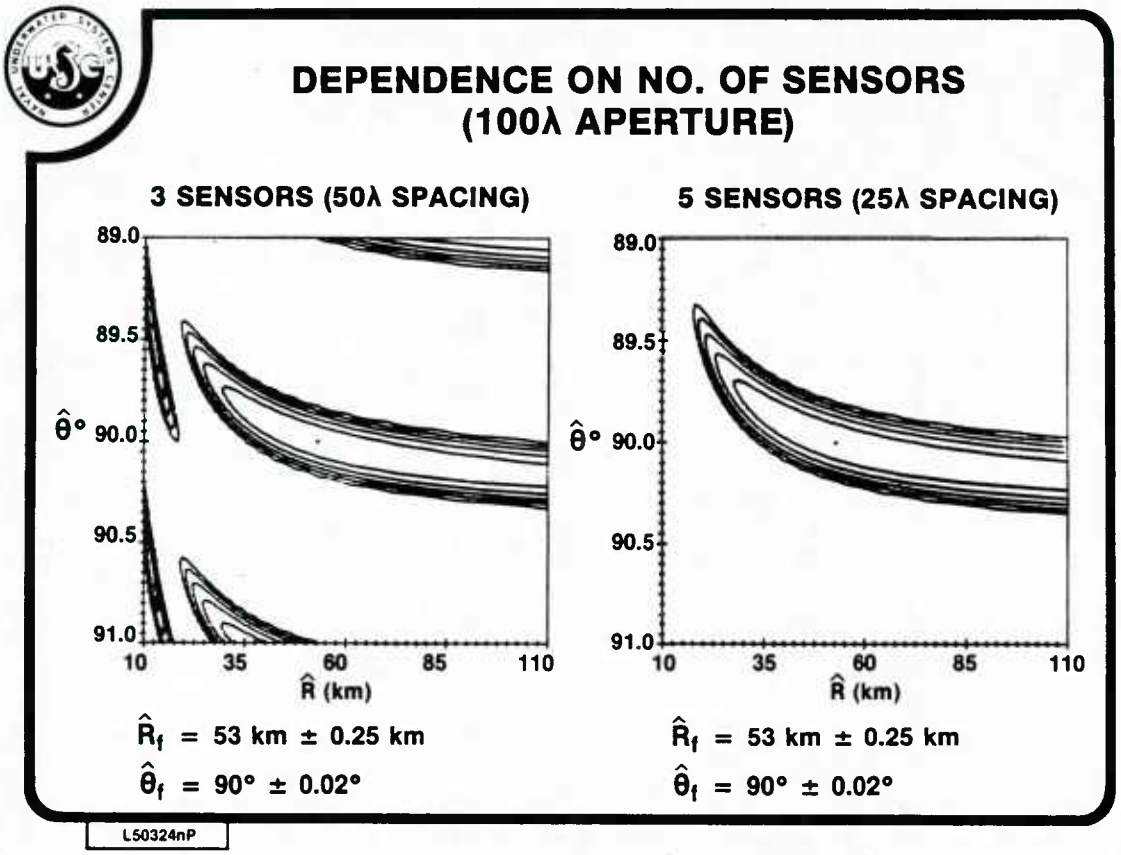

Viewgraph 10

The dependence of the estimator outputs on the number of sensors for a fixed array length is shown here. The nature of the dependence in this case can be explained on the basis of array response functions. As we fill in the array with more sensors, we expect to spread out the grating lobes. In addition, near the array a higher order summation in the beamformer tends to reduce the level of the interference patterns occurring at close range. Therefore, we note the inclusion of a multipath environment has had little impact on the estimator outputs.

-- Next viewgraph, please. --

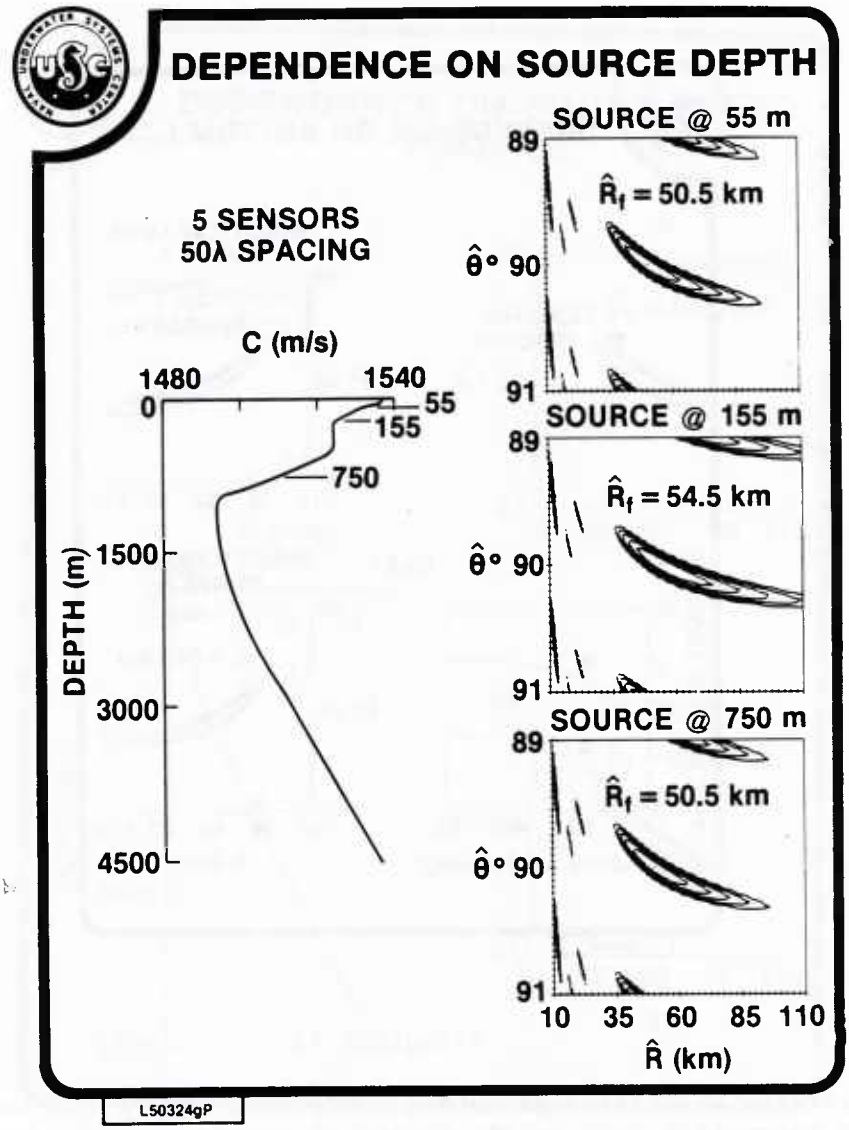

Viewgraph 11

This viewgraph illustrates the dependence of the estimator output on the depth at which the source is located. For this comparison we are using a 5-sensor array with an interelement spacing of 50λ and has a hyperfocal range of about 70 kilometers. Thus, for a source at 50 kilometers we can expect closed contours as seen here. The three source depths of 55, 155, and 750 meters are shown in relation to the typical North Atlantic sound speed profile on the left side of this viewgraph. We note there is little difference between the contours for the shallowest and deepest source depth. There are, however, two things worth noting. When the source is at 155 meters a larger area is enclosed by the highest level contour and the local maximum is farther from the actual range than for the other two depths. An analysis of the eigenray structure reveals that the multipath structure is more complicated for the 155-meter source depth than at 55 or 750 meters. Thus, it is reasonable to expect less accurate results for a source depth of 155 meters.

-- Next viewgraph, please. --

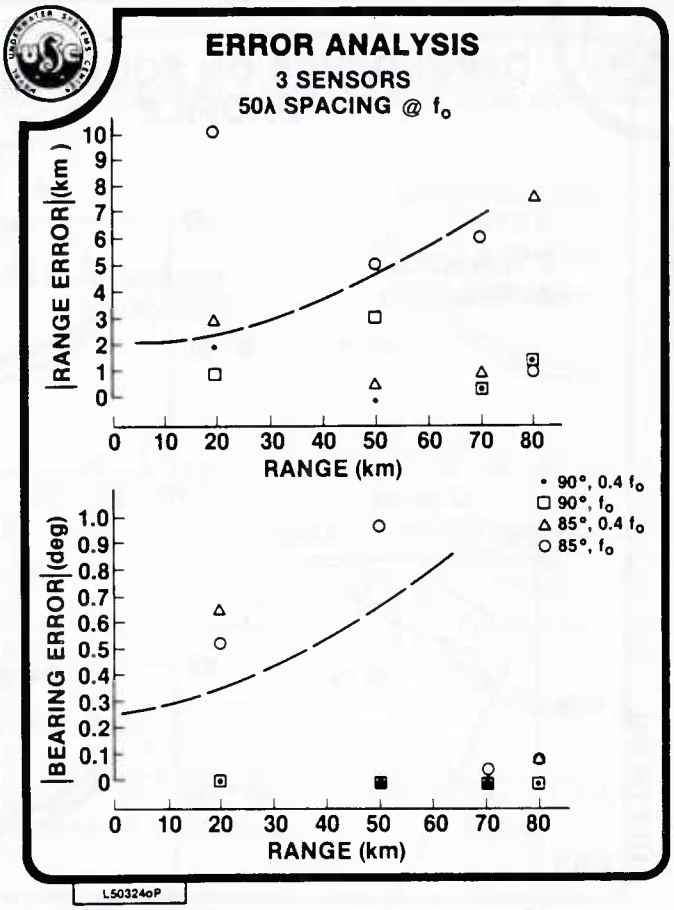

Viewgraph 14

For direct path propagation there are no errors introduced in the estimation of source location for range or bearing. We have just shown that for our set of parameters that when multipath conditions exist there are errors introduced. These errors are a function of the complexity of the acoustic multipath structures. Shown here are the absolute range and bearing error versus range for bearing angles of 90 and 85 degrees and two frequencies.

Overall, the multipath simulations at a broadside bearing angle indicate good bearing and range estimates as a function of range and frequency. When the off-broadside cases are analyzed, more error is seen. The off-broadside range error has been examined in a recent study by Wood [7], and a correction factor presented for single path propagation.

The dashed lines in these two figures represent a crossover point where the maximum likelihood estimator has shifted source estimation from the main lobe to an ambiguous bearing lobe. This is noted by the occurrence of large absolute bearing errors. The shifting of source location to an ambiguous peak not only introduces large bearing errors, but large absolute range errors as well. We see the shifting to an ambiguous peak only occurred for some of the off-broadside cases and appears to have no frequency dependence.

-- Next viewgraph, please. --

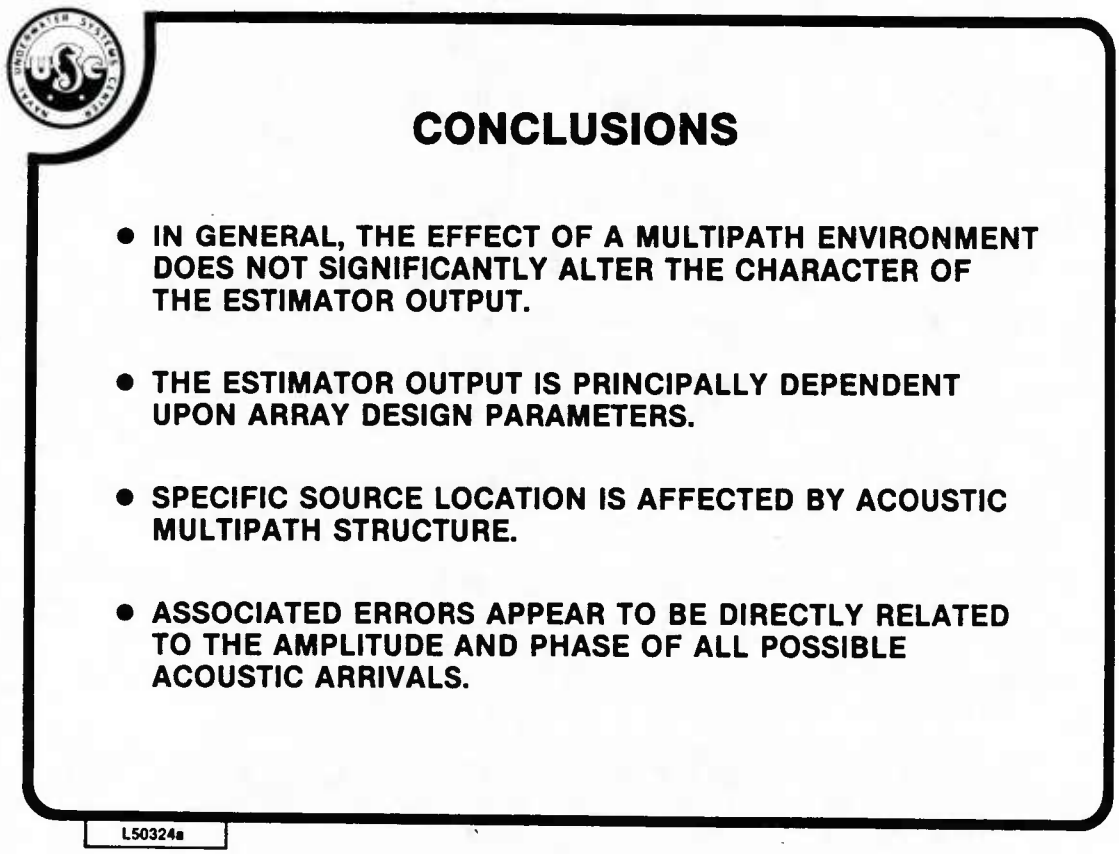

Viewgraph 15

In conclusion overall inspection of the contour plots of array estimator output in a multipath environment show small variations as a function of engineering and environmental parameters. It is apparent that as the frequency decreases, the number of ambiguity surfaces in bearing also decreases. Also, the addition of more sensors decreases the interelement spacing, which decreases the ambiguity in bearing. However, the environmental parameters dictate the complexity of the multipath structure and the effectiveness of the estimation process is directly related to the acoustic multipath.

REFERENCES

1. G. Clifford Carter, "Time Delay Estimation for Passive Sonar Signal Processing," IEEE Transactions on Acoustics, Speech, and Signal Processing, Vol. ASSP-29, No. 3, June 1981, pp. 463-470.

2. Joseph C. Hassab, "Passive Bearing Estimation of a Broad-Band Source," IEEE Transactions on Acoustic, Speech, and Signal Processing, Vol. ASSP-32, No. 2, April 1984, pp. 426-431.

3. Kenneth B. Theriault and Robert M. Zeskind, "Inherent Bias in Wavefront Curvature Ranging," IEEE Transactions on Acoustics, Speech, and Signal Processing," Vol. ASSP-29, No. 3, June 1981, pp. 524-526.

4. Norman L. Owsley and Gerald R. Swope, "Time Delay Estimation in a Sensor Array," IEEE Transactions on Acoustics, Speech, and Signal Processing, Vol. ASSP-29, No. 3, June 1981, pp. 519-523.

5. Henry Weinberg, Generic Sonar Model, NUSC Technical Document 5971C, Naval Underwater Systems Center, New London, CT, 15 December 1981.

6. Bernard D. Steinberg, Principles of Aperture and Array System Design, John Wiley and Sons, Inc., NY pp 40-59.

7. David H. Wood, Measuring Normal Curvature of Wavefronts, NUSC Technical Report 7009, Naval Underwater Systems Center, New London, CT (in preparation).

INITIAL DISTRIBUTION LIST

Addressee	No. of Copies
CNO (CDR H. Dantzler, 952D)	1
NAVELECSYSCOM (ELEX 612: R. Mitnick, J. Schuster, B. Ogg; PME-124, L. Parish)	4
NAVSEASYSCOM (SEA-63R: C. Smith, D. Porter, J. Shooter, D. Barbour, D. Early; -63D, T. Tiedieman)	5
NAVPGSCOL	1
DWTNSRDC	1
NORDA (113, 200, 220, 240, 245, 260, 270, Library)	8
NOSC (7133: D. Persons, J. McCarthy; R. Smith, H. Bucker, Library)	5
NADC (P. Haas, B. Sternberg, Library)	3
NSWC (M. Williams, R. Stevenson, Library)	3
NRL (5160: R. Dicus, R. Doolittle; Library)	3
SACLANTCEN (R. Goodman, E. Sullivan, T. Goldsberry, Library)	4
DARPA (C. Stuart)	1
CNM (T. Warfield)	1
Defense Research Establishment Pacific (D. Thomson, J. Syck)	2
FWG (H. Herwig, B. Nuetzel, G. Ziehm)	3